VOL. 4, NO. 1, FEBRUARY 2009 ISSN 1819-6608
ARPN Journal of Engineering and Applied Sciences


www.arpnjournals.com

SIMULATION OF IN-CYLINDER PROCESSES IN A DI DIESEL ENGINE WITH VARIOUS INJECTION TIMINGS

S. M. Jameel Basha[1], P. Issac Prasad[2] and K. Rajagopal[3]
[1]Mechanical Engineering Department, Intell Engineering College, Anantapur, A. P., India
[2]Mechanical Engineering Department, Koneru Lakshmaiah College of Engineering, Vijayawada, A. P., India
[3]Mechanical Engineering Department, JNT University, Hyderabad, A. P., India
E-Mail: jameel_junaid@yahoo.com; Prasadissac2002@yahoo.co.in

ABSTRACT

The gas motion inside the engine cylinder plays a very important role in determining the thermal efficiency of an internal combustion engine. A better understanding of in cylinder gas motion will be helpful in optimizing engine design parameters. An attempt has been made to study the combustion processes in a compression ignition engine and simulation was done using computational fluid dynamic (CFD) code FLUENT. An Axisymmetric turbulent combustion flow with heat transfer is to be modeled for a flat piston 4-stroke diesel engine. The unsteady compressible conservation equations for mass (Continuity), axial and radial momentum, energy, species concentration equations can express the flow field and combustion in axisymmetric engine cylinder. Turbulent flow modeling and combustion modeling was analyzed in formulating and developing a model for combustion process.

1. INTRODUCTION

The Modeling of a process has come to mean developing and using the appropriate combination of assumptions and equations that permit critical features of the process to be analyzed. The new and changing requirements demanded by the market have greatly increased the complexity of engine design to give optimum operating characteristics to the fuel economy and limitations in emissions models that are being developed and used to describe engine operating and emission characteristics can be categorized as thermodynamic or fluid dynamic in nature, depending on weather the equations which give the model its predominant structure and based on energy conservation or a full analysis of the fluid motion engine combustion models are classified as

- Thermo dynamic based models (Zero dimensional models)
- Fluid dynamic based models (Multi dimensional models)

The new dimensional models usually refer to a thermodynamic analysis of the engine cycle where charge is assumed to be uniform in composition. These models are not realistic in nature.

Fluid dynamic based models are often called as multi dimensional models due to their inherent ability to provide detailed information of the spatial distribution of gas velocity and other characteristics of the flow within the engine cylinder [2]. These models are realistic in nature and are able to take care of the combustion chamber geometries.

1.1 Scope of present work

It is evident from the foregoing discussion that multidimensional calculations for the in cylinder flows are proved to be powerful tool as diesel engines are widely used now a days.

A two dimensional Axisymmetric model has been chosen for this investigation. The turbulence model and combustion model has been taken for analysis. The turbulence and combustion models used are made as clear as possible to capture the real process. The three dimensional model with changed piston geometry, injection, valve motor would demand greater computer capabilities for analysis.

1.2 CFD Analysis

CFD codes are structured around the numerical Algorithms that can tackle fluid flow problems. In order to provide easy access to their solving power all commercial CFD packages include sophisticated user interfaces to input problems parameters and to examine the results. Hence all codes contain three main elements.

A pre-processor (ii) a solver and (iii) a post-processor

Pre-processor

The user activities at the pre-processing stage involve:

- Definition of the geometry of the region of interest: The computational domain.
- Grid generation-The sub division of the domain in to a number of smaller non overlapping sub domains : a grid (or mesh) of cells.
- Selection of the physical and chemical phenomena that need to be modeled.
- Definition of fluid properties.
- Specification of appropriate boundary conditions at cells which coincide with or touch the domain boundary.

The accuracy of a CFD solution is governed by the number of cells in the grid. In general, the larger the number of cells, the better the solution accuracy.

Solver

There are three distinct streams of numerical solution techniques: finite difference, finite element and spectral methods. The outline numerical algorithm consists of the following step:

- Integration of the governing equations of fluid flow over all the control volumes of the domain.
- Discritization- conversion of the resulting integral equations into a system of algebraic equations
- Solution of the algebraic equations by an iterative method.

Post-Processor

The post processing consists of:

- Domain geometry and grid display
- Vector plots
- Line and shaded contour plots
- 2D and 3D surface plots
- Particle tracking
- View manipulation
- Color post script output

Gambit has been used as geometry creation and mesh generation software (pre-processor). Fluent has been used as a solver and post-processor.

1.3 Gambit

Geometry can be made using the pre-processor. The software is designed to build mesh models for CFD and other scientific applications. The gambit GUI makes the basic step of building and meshing a model.

1.4 Fluent

FLUENT provides complete mesh flexibility solving flow problems with unstructured meshes that can be generated about complex geometry with relative ease [3]. FLUENT allows refining or coarsening grid based on the flow simulation. The files in the FLUENT are written in C-language. It ensures complete mesh flexibility by using unstructured quadrilateral / hexagonal, triangular / tetrahedral or hybrid meshes with solution based mesh adoption.

2. NUMARICAL MODELLING

In the present work, the turbulence was accounted using K- ε model.

2.1 K- ε model of turbulence

The K- ε model for solving Navier stoke's equation employees the eddy viscosity concept. It however estimates μ using principle of energy balance in the turbulent microstructure rather than algebraic formulae. Since K and ε both are produced destroyed and transported by flow, one obtains partial differential equations governing their values in the flow domain.

2.2 Flow field in Ax symmetric coordinates

Overall continuity equation

$$\frac{\partial \rho}{\partial t}+\frac{\partial(\rho u)}{\partial z}+\frac{1}{r}\frac{\partial(\rho r v)}{\partial r}=\dot{\rho}_{fu}^{s}$$

2.3 Axial momentum equations

$$\frac{\partial(\rho u)}{\partial t}+\frac{\partial(\rho uu)}{\partial z}+\frac{1}{r}\frac{\partial(\rho uvr)}{\partial r}=\frac{\partial\left(\mu_{eff}\frac{\partial u}{\partial z}\right)}{\partial z}+\frac{1}{r}\frac{\partial\left(r\mu_{eff}\frac{\partial u}{\partial r}\right)}{\partial r}+S_u$$

Where $\mu_{eff}=\mu+\mu_t$

$\mu=1.78\times10^{-5}\ Ns/m^2$

$$\mu_t=C_\mu\rho\frac{k^2}{\varepsilon}$$

$C_\mu=0.09$

$S_u=-\frac{\partial p}{\partial z}+\frac{\partial\left(\mu_{eff}\frac{\partial u}{\partial z}\right)}{\partial z}+\frac{1}{r}\frac{\partial\left(r\mu_{eff}\frac{\partial v}{\partial z}\right)}{\partial r}-\frac{2}{3}\frac{\partial\left(\mu_{eff}\nabla.V+\rho k\right)}{\partial z}+F_u^s$ and

$\nabla.V=\frac{\partial u}{\partial z}+\frac{1}{r}\frac{\partial(vr)}{\partial r}$

2.4 Radial momentum equation

$$\frac{\partial(\rho v)}{\partial t}+\frac{\partial(\rho uv)}{\partial z}+\frac{1}{r}\frac{\partial\left(\rho v^{2r}\right)}{\partial r}=\frac{\partial\left(\mu_{eff}\frac{\partial v}{\partial z}\right)}{\partial z}+\frac{1}{r}\frac{\partial\left(r\mu_{eff}\frac{\partial v}{\partial r}\right)}{\partial r}+S_v$$

Where

$S_v=-\frac{\partial p}{\partial r}+\frac{\partial\left(\mu_{eff}\frac{\partial u}{\partial r}\right)}{\partial z}+\frac{1}{r}\frac{\partial\left(r\mu_{eff}\frac{\partial v}{\partial r}\right)}{\partial r}-2\mu_{eff}\frac{v}{r^2}-\frac{2}{3}\frac{\partial\left(\mu_{eff}\nabla.V+\rho k\right)}{\partial r}+F_v^s$

2.5 Turbulent kinetic energy (k)

$$\frac{\partial}{\partial t}(\rho k)+\frac{\partial}{\partial z}(\rho uk)+\frac{1}{r}\frac{\partial}{\partial r}(\rho rvk)=\frac{\partial}{\partial z}\left(\frac{\mu_{eff}}{\sigma_k}\frac{\partial k}{\partial z}\right)+\frac{1}{r}\frac{\partial}{\partial r}\left(r\frac{\mu_{eff}}{\sigma_k}\frac{\partial k}{\partial r}\right)+S_k$$

Where

$\sigma_k=1.0$

$S_k=G-\rho\varepsilon$

$G=2\mu_{eff}\left(\left(\frac{\partial u}{\partial z}\right)^2+\left(\frac{\partial v}{\partial r}\right)^2+\left(\frac{v}{r}\right)^2+\frac{1}{2}\left(\frac{\partial u}{\partial r}+\frac{\partial v}{\partial z}\right)^2\right)$

2.6 Turbulent kinetic energy dissipation rate

$$\frac{\partial}{\partial t}(\rho\varepsilon)+\frac{\partial}{\partial z}(\rho u\varepsilon)+\frac{1}{r}\frac{\partial}{\partial r}(\rho rv\varepsilon)=\frac{\partial}{\partial z}\left[\frac{\mu_{eff}}{\sigma_\varepsilon}\frac{\partial\varepsilon}{\partial z}\right]+\frac{1}{r}\frac{\partial}{\partial r}\left(\frac{r\mu_{eff}}{\sigma_\varepsilon}\frac{\partial\varepsilon}{\partial r}\right)+S_\varepsilon$$

Where

$S_\varepsilon=\frac{\varepsilon}{k}\left(C_1G-C_2\rho\varepsilon\right)+C_3\rho\varepsilon\nabla.V$

$$\sigma_\varepsilon = \frac{k^2}{(C_2 - C_1)C_\mu^{1/2}} = 1.2$$

$C_1 = 1.44$

$C_2 = 1.92$

$k = 0.4$

$C_3 = -1/3 \backslash$

2.7 General transport equations

All the above equations can be represented compactly by a more general transport equation in terms of primitive variable ϕ as:

$$\frac{\partial}{\partial t}(\rho\phi) + \frac{\partial}{\partial z}(\rho u\phi) + \frac{1}{r}\frac{\partial}{\partial r}(\rho rv\phi) = \frac{\partial}{\partial z}\left(\Gamma_\phi \frac{\partial \phi}{\partial z}\right) + \frac{1}{r}\frac{\partial}{\partial r}\left(r\Gamma_\phi \frac{\partial \phi}{\partial r}\right) + S_\phi$$

Where $\phi = u, v, k, \varepsilon, m_{fu}, T, f$ $S_\phi =$

Corresponding source term.

Γ_ϕ = Corresponding diffusion coefficient

2.8 Initial boundary condition

In the problem one of the boundaries of the flow domain (piston head) is in motion. Therefore, the need arises for transforming the conservation equations to a co-ordinate system which moves with the moving with the moving boundary.

There fore the co-ordinate is transformed from (r,t,z) to

(r, t, ξ) Co-ordinate system, where,

$$\xi = \frac{z}{z_p}$$

z_p Being the instantaneous piston displacement.

The equations for instantaneous piston position (z_p) and the instantaneous piston velocity (u_p) are expressed below:

$$z_p = C + l(1 - \cos(\theta)) + L\left[1 - \sqrt{1 - \left(\frac{l}{L}\sin(\theta)\right)^2}\right]$$

$$u_p = \omega l\left[\sin(\theta) + \frac{l}{2}\frac{\sin(2\theta)}{\sqrt{L^2 - (L\sin(\theta))^2}}\right]$$

Where

$\theta = \omega t$,

C is the clearance, θ the crank angle, ω is the angular velocity in radians per second, l is the half stroke length and L is the connecting rod length.

The general transport equation in transformed co-ordinates is given by

$$\frac{1}{z_p}\frac{\partial}{\partial t}(\rho z_p\phi) + \frac{1}{z_p}\frac{\partial}{\partial \xi}(\rho u_\xi \phi) + \frac{1}{r}\frac{\partial}{\partial r}(\rho rv\phi) - \frac{1}{z_p}\frac{\partial}{\partial \xi}\left(r\Gamma_\phi \frac{\partial \phi}{\partial r}\right) = \bar{S}_\phi$$

$\bar{S}_\phi$ Is the transformed source term for a given ϕ.

$u_\xi = (u - \xi u_p)$, and u_p is the piston velocity.

Equation of state

In this analysis, the ideal gas equation of state is used. So the density is given by

$$\rho = \frac{p}{RT}$$

Where,

$$R = \sum_{i=1}^{n} m_i R_i$$

$R_i = \frac{\bar{R}}{W_i}$ $\bar{R}$ = Universal gas constant

W_i = Molecular weight of species i.

3. METHODOLOGY

3.1 Simulation assumptions

- Perfect gas laws were used for analysis
- Swirl effect is neglected
- Combustion is assumed to be stoichiometric and reaction rate infinitely fast
- All the fuel injected vaporizes and combustion products are formed.

3.2 Predictive capability

The FLUENT package has an advantage of nicely capturing the physics of the in cylinder combustion process. The in cylinder flow pattern and temperature profiles during the entire process, with turbulence levels and pressure distributions all confirm to the practical expectations. The key factor in determining the combustion rate is the relative concentrations of the fuel and oxygen at any discrete location inside the cylinder.

3.3 Engine geometry and simulation

In the present work flat headed piston was modeled in gambit and imported. The compression and expansion strokes were analyzed. Injection was done at various injection timings such as 9°, 18° and 25° before TDC. An axisymetric turbulent combustion flow was modeled using K – ε model which uses eddy viscosity concept. A modeled hexagonal grid is presented in Figure-1.

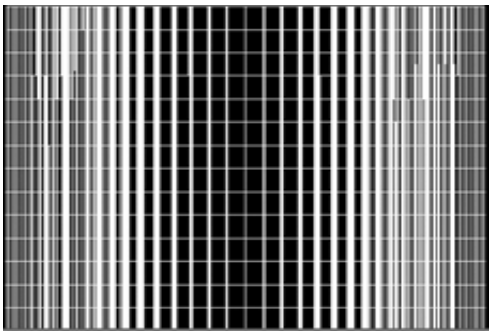

Figure-1. figure showing full hexagonal grid.

3.4 Initial conditions

The simulation is initialized for the start of injection at 9°, 18°, 25° before TDC. The total duration of Injection is 20° from start of injection. The fuel used is n-heptane (C7 H16) the quantity of fuel injected is 30 mg per cycle and injection made was constant as 1.2 mg per unit crank angle. The initial fuel temperature was taken as 313° K the diameter as injected nozzle is 0.2mm the model engine specifications are listed in Table-1.

Table-1. Specifications of model engine.

Cylinder bore	78 cmϕ
Piston crown	Flat
Engine speed	2400 rpm
Compression stroke	15.1 cm
Fuel	n-Heptane
Fuel temperature	313° k
Duration of injection	20°
Injection Nozzle orifice diameter	0.2 mm
Injection pressure	25 MPa
Injected fuel quantity	30 mg / cycle

4. RESULTS AND DISCUSSIONS

4.1 Analysis of results

The results presented pertain to compression and expansion strokes. The runs were made using a hexagonal grid with injection at different crank angles and with fixed quantity of mass. The time step used in 1° crank angle for fluid flow without combustion and during combustion. The results were presented with injection at different crank angles and without varying of quantity of fuel injected.

Figures 2, 3 and 4 show the contours of static pressures. The figures were shown for the injection timings of 9°, 18° & 25° BTDC. The figures presented were taken when the piston is at 10° after TDC. The maximum pressure accurse when the injection was done at 18° before TDC.

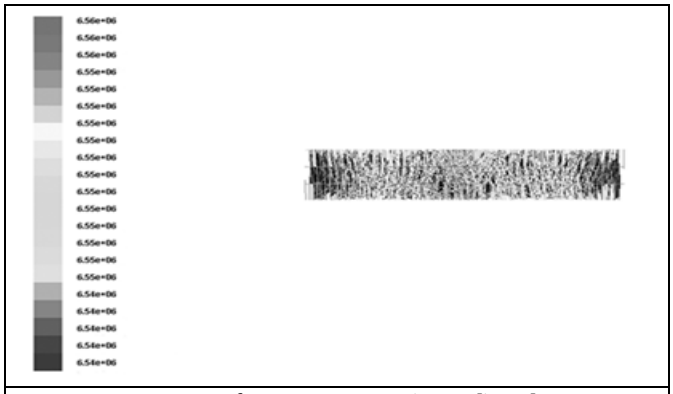

Contours of static pressure (Pascal), July 27, 2008
FLUENT 6.2 (3d, dp, segregated, dynamesh, df18, rngke, unsteady)

Contours of static pressure (Pascal) (Time = 1.2917e-02)
Jul 27, 2008
FLUENT 6.2 (3d, dp, segregated, dynamesh, df18, rngke, unsteady)

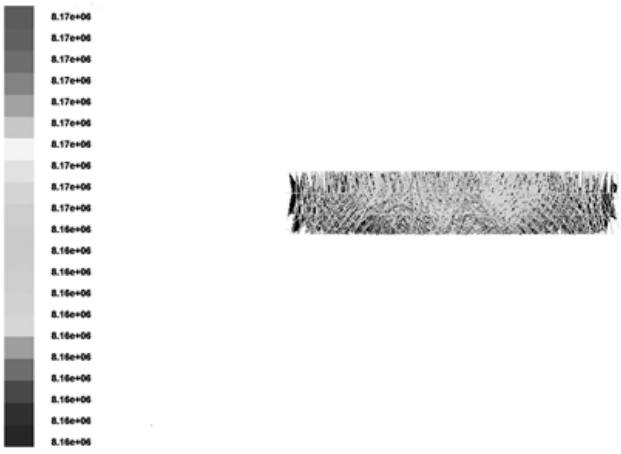

Contours of static pressure (Pascal) Jul 27, 2008
FLUENT 6.2 (3d, dp, segregated, dynamesh, df18, rngke, unsteady)

Figures 2, 3 and 4. Contours of static pressure for 9°, 18° and 25° Injection timings.

Figures 5, 6 and 7 show the contours of turbulence kinetic energy for the injection timing of 9°,

18° & 25° BTDC. From the figures it is evident that TKE is higher for injection at 18° before TDC.

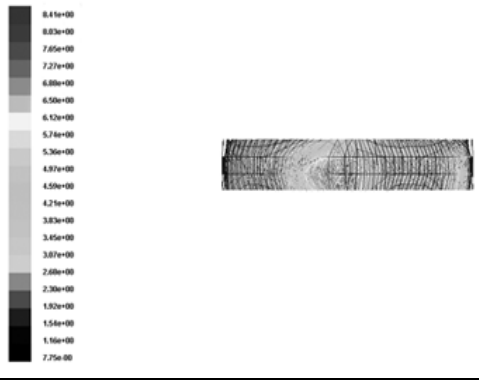

Contours of turbulence kinetic energy (k) (m2/s2)
(Time = 1.3264e-02) Jul 27, 2008
FLUENT 6.2 (3d, dp, segregated, dynamesh, df18, rngke, unsteady)

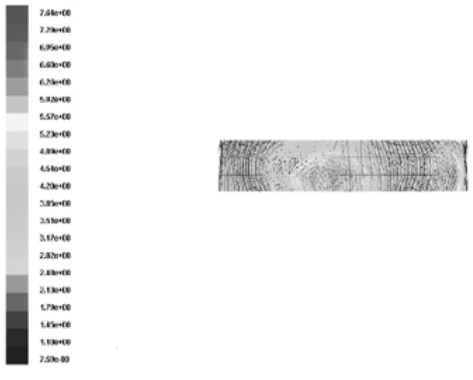

Contours of turbulence kinetic energy (k) (m2/s2)
(Time = 1.3264e-02) Jul 27, 2008
FLUENT 6.2 (3d, dp, segregated, dynamesh, df18, rngke, unsteady)

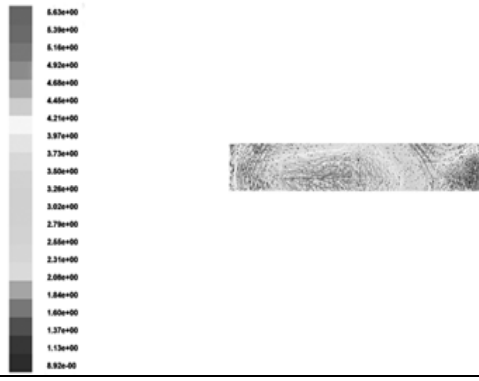

Contours of Turbulence Kinetic Energy (k) (m2/s2)
(Time=1.2917e-02) Jul 27, 2008
FLUENT 6.2 (3d, dp, segregated, dynamesh, df18, rngke, unsteady)

Figures 5, 6 and 7. Contours of turbulence kinetic energy for 9°, 18° and 25° Injection timings.

4.2 In-cylinder pressure and temperature during combustion

The results are analyzed at three different points of injections (i.e. 9°, 18° and 25° BTDC) keeping fuel injected at all injection points as constant (i.e. 30mg). Also fuel injection rate was made constant as 1.2 mg per unit crank angle. The duration of injection for each case is 25° of crank Angle.

At the start of combustion after the ignition delay there is a sudden change of slope of the p-θ curve. The pressure rises rapidly for a few crank angle degrees, and then moves slowly towards a peak value.

For the start of injection at 25° BTDC the peak pressure is noticed 2° after TDC for injection at 18° BTDC the peak pressure is attained 4° after TDC, injection at 9° BTDC the peak pressure is attained 10° after TDC (Figure-8)

The temperature diagram reveals a maximum bulk temperature of 2021K at 25° injection point, 2020K at 18° injection point and 1754 K at 9° injection point. For all the aforesaid cases the maximum temperature is obtained after attainment of the peak pressure (Figure-9).

4.3 In-cylinder turbulence kinetic energy, dissipation rate and intensity during combustion

The Turbulent Kinetic Energy (T.K.E.) is noticed to be different with injection timing. The TKE is slightly higher for 9˚ BTDC injection as compared to injection at 18˚ BTDC. However, a considerable variation in TKE is noticed when fuel injection occurs at 25˚ BTDC. The TKE for this case is considerably low as compared to injection at 9° and 18° BTDC (Figure-10). Figure-11 shows the turbulent kinetic energy dissipation rate. A sharp raise in dissipation rate is noticed when the piston is approaching top dead centre. For fuel injection at 18˚ and 25˚ BTDC when the piston reaches TDC there is fall of dissipation rate but grater fall is noticed incase of injection timing at 25˚ BTDC. This is attributed to the fact that the injection was done only for the duration of 20˚ from the start of injection. Incase of 25˚ start of injection, the injection completes 5˚ before TDC where as incase of 18 start of injection, the injection will continue until 7˚ after TDC. Further dissipation rate increases as the piston moves up and reaches its maximum value when the piston is at the end of compression stroke. For 9˚ start of injection though there is less increase in dissipation rate when the piston is approaching TDC, after TDC there is steep raise in dissipation rate. Figure-12 represents turbulence intensity.

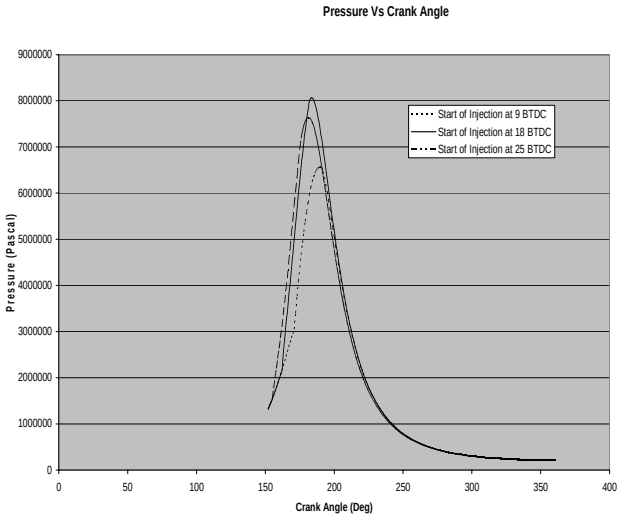

Figure-8. Pressure vs. Crank angle.

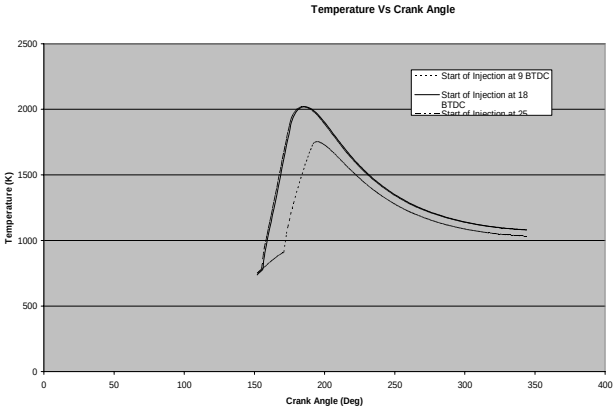

Figure-9. Temperature vs. Crank angle.

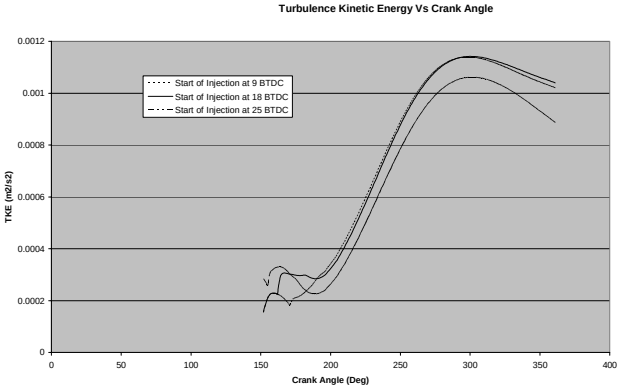

Figure-10. Turbulence kinetic energy vs. Crank angle.

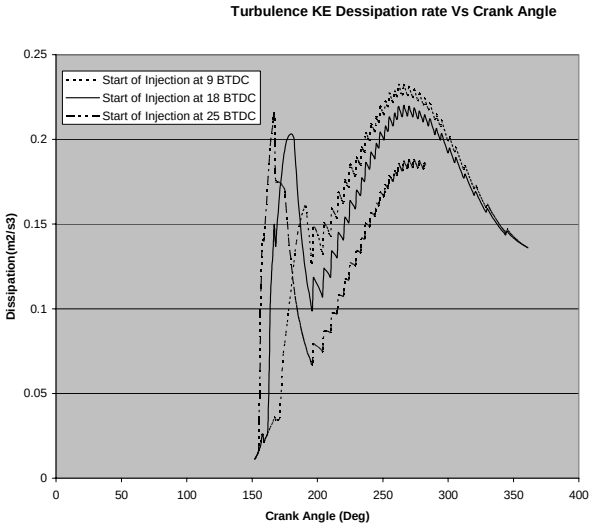

Figure-11. Turbulence dissipation rate vs. Crank angle.

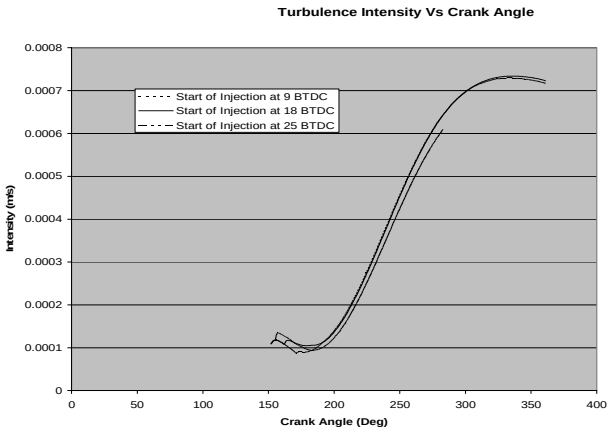

Figure-12. Turbulence intensity vs. Crank angle.

5. CONCLUSIONS

A detailed CFD model for predicting the fluid flow and combustion was developed. It is concluded from this study that the injection of fuel at 18˚ before TDC is effective. It was observed that there is reasonable growth in the pressure, temperature, turbulence kinetic energy by starting the injection at 18˚ BTDC. It will be interesting to study the simulation if the mass of the fuel injected is varied.

REFERENCES

[1] John B. Heywood. Internal Combustion Engine Fundamentals. MC-Graw Hill International Editions.

[2] Huh K.Y. and Gosman A.DA. 1991. Phenomenological model of diesel spray atomization. Proceedings of the International Conference on multiphase flows. ICMF.

[3] FLUENT 6.1.22. 2003. User's manual and tutorial guide, Fluent Inc., USA.

[4] Bai C. and Gosman A.D., "Development of Methodology for spray impingement simulation". SAE Technical paper series 950283.

[5] Philip Adomeit, Oliver Lang, Reiner Schulz and Volker Weng FD. 2002. "Simulation of direct injection and combustion". SAE Technical Paper, 2002-01-0945.